# Deletion of PLD2 Alleviates LPS Induced Acute Lung Injury by Inhibiting STAT3 Phosphorylation and Regulating Endothelial Tight Junctions

**Tiantian Qian**
Binzhou Medical University Hospital
**Boyang Qi**
Yantai yuhuangding Hospital of Qingdao University Medical College
**Yuxin Fei**
Binzhou Medical University Hospital
**Jun Li**
Yantai Affiliated Hospitol of Binzhou Medical University
**Liqing Luo**
Binzhou Medical University Hospital
**Yutong Song**
Binzhou Medical University Hospital
**Shurui Sheng**
Binzhou Medical University Hospital
**Bingjie Lv**
Binzhou Medical University Hospital
**Xiao Huang**
Binzhou Medical University Hospital
**Xiaozhi Wang** ( hxicuwxz@163.com )
Binzhou Medical University Hospital

**Research Article**

**Keywords:** Acute respiratory distress syndrome , Acute lung injury, Phospholipase D2, STAT3, Tight junction proteins

**Posted Date:** June 10th, 2022

**DOI:** https://doi.org/10.21203/rs.3.rs-1641656/v2

# Abstract

**Background:** Acute respiratory distress syndrome (ARDS) is the leading cause of acute respiratory failure. Endothelial cell damage and increased permeability are critical in developing acute lung injury (ALI). Phospholipase D2 (PLD2) and its metabolite phosphatidic acid (PA) regulate many physiological activities in cells, disrupting cell barrier integrity. However, the exact mechanism remains unexplored. Therefore, we elucidated the role and action mechanism of PLD2 in lipopolysaccharide (LPS)-induced endothelial cell integrity.

**Methods:** We used wild-type (WT) and PLD2 knockout ($PLD2^{-/-}$) mouse models of LPS-induced ALI. Altered pulmonary endothelial permeability was assessed using histopathological analysis. The relative permeability of the pulmonary vascular endothelial cell culture model was assessed using transwell chamber assays for FITC-dextran and TEER transcellular resistance. The PA content, a downstream product of PLD2, was detected using ELISA, and the mRNA expression of tight junction proteins was detected by real-time quantitative polymerase chain reaction (RT-PCR). Changes in tight junction protein levels and STAT3 pathway phosphorylation, a critical endothelial barrier component, were assessed using immunofluorescence and western blotting analyses in vivo and in vitro.

**Results:** $PLD2^{-/-}$ could significantly improve the histopathological changes, lung wet-dry ratio, and endothelial cell permeability in LPS-induced ALI mice. Simultaneously, $PLD2^{-/-}$ could reduce PA-induced STAT3 phosphorylation, resulting in reduced endothelial tight junction degradation.

**Conclusion:** Loss or inhibition of PLD2 significantly inhibits tight junction injury and alleviates lung injury. LPS-induced PA production leads to STAT3 pathway phosphorylation and tight junction protein targeting, resulting in increased barrier permeability. Collectively, PA is crucial in ARDS pathogenesis.


# 1. Introduction

ARDS, an inflammatory lung condition characterized by an acute onset and arterial hypoxia with bilateral pulmonary infiltrates, is a common cause of respiratory failure in critically ill patients. ARDS arises as a complication of other primary diagnoses, such as sepsis, pneumonia, trauma, aspiration of gastric contents, or multiple transfusions [1, 2]. ARDS is present in approximately 10% of intensive care unit patients worldwide, and mortality remains as high as 30–40% in most studies [3]. Although numerous studies have focused on the mechanisms and treatment strategies of ARDS, effective therapies to minimize the profound vascular leakage in ARDS are not currently available, and significant morbidity and mortality in critically ill patients are a major clinical problem [4, 5]. Pathologic examination of patients commonly reveals diffuse alveolar damage (DAD), and laboratory studies have shown diffuse alveolar-capillary injury and increased vascular permeability, leading to the accumulation of protein-rich inflammatory edema fluid in the alveolar space. Studies on pulmonary vascular endothelial cell permeability are essential for understanding the mechanism of ARDS because these cells exert multiple

relevant effects, such as generating inflammatory mediators and regulating intracellular adhesion, which are related to the endothelial barrier [6].

The endothelial barrier, a physical barrier formed by pulmonary endothelial cells and tightly connected intercellular complexes, may play a key role in ARDS. Tight junctions play dual roles as barriers and fences, which are essential for the development and maintenance of multicellular organisms. They create a primary barrier to the diffusion of solutes through the paracellular pathway. They are thought to maintain cell polarity as a boundary between the apical and basolateral plasma membrane domains [7]. At least three transmembrane proteins are required to construct tight junction complexes: occludin, zonula occludens protein-1 (ZO-1), and claudin-1 [8]. Occludin and ZO-1 are bridges between tight junctions and cytoskeletal proteins and play a vital role in permeability and inflammation. Damage to occludin and ZO-1 results in alveolar exudate formation and attenuates its clearance [9–13].

Phospholipase D2 (PLD2) is a lipid-signaling enzyme regulating several cellular events. The classic function of PLD2 catalyzes the hydrolysis of phosphatidylcholine (PC) to produce the signal molecule phosphatidic acid (PA) [14]. The molecular characteristics of PLD2, the mechanisms of regulating its activity, its functions in the signaling pathway involving PA and its binding partners, and its role in cellular physiology have been extensively studied over the past decades [15]. Various cellular stimuli can activate PLD2 to generate PA, which mediates various cellular events and signaling pathways, depending on the stimuli and cellular context. Although several potential roles of PLD2 have been proposed based on molecular and cell-based studies, the pathophysiological functions of PLD2 in vivo have not yet been comprehensively investigated at the organismal level [16–18].

The signal transducer and activator of transcription (STAT) proteins are a family of cytoplasmic transcription factors which share an overall general structure, organized into functional modular domains. The mammalian STAT family comprises STAT1, STAT2, STAT3, STAT4, STAT5a, STAT5b, and STAT6, which mediate multiple intracellular signaling pathways [19]. Among them, the transcriptional regulator STAT3 plays a crucial role in vertebrate development and mature tissue function, including the control of inflammation and immunity [20], and participates in many biological processes such as cell proliferation, survival, differentiation, and angiogenesis. In normal cells, the transient activation of STAT3 (mainly through phosphorylation) transmits the transcription signals of cytokines and growth factor receptors on the plasma membrane to the nucleus. Targeting the STAT3 signaling pathway is a promising treatment strategy [19, 21–24].

This study aimed to explain the role and action mechanism of PLD2 on LPS-induced endothelial cell integrity. To test the hypothesis that PLD2 is a critical regulator of the tight junction proteins occludin and ZO-1, we used PLD2 ($PLD2^{-/-}$) knockout mice and human umbilical vein endothelial cells (HUVECs) to study the effect of altered PLD2 expression or PA levels on endothelial cell permeability. We observed that PLD2 deficiency reduced acute lung injury (ALI) severity and was associated with decreased vascular endothelial barrier permeability. Additionally, PLD2 inhibition attenuated PA-induced STAT3 phosphorylation, and the STAT3 signaling pathway negatively regulated the expression levels of occludin

and ZO-1. Collectively, our data suggest that blocking PLD2 can improve ARDS symptoms, and PLD2 may be a therapeutic target in ARDS.

# 2. Methods

## 2.1 Animals Studies

PLD2$^{-/-}$ mice on a C57BL/6 background were purchased from Gempharmatech Co., Ltd. (Jiangsu, China), and Male C57BL/6 mice (WT) (18–23 g; 8–10 weeks old) were purchased from Jinan Pengyue Laboratory Animal Breeding Co., Ltd. (Shangdong, China) and housed in a room maintained at 22–25°C and 40–50% humidity. Food and water were available ad libitum. All animal experiments and feeding methods complied with the guidelines for the Care and Use of Laboratory Animals established by the US National Institutes of Health and were approved by the Binzhou Medical University Institutional Review Board.

Experimental mice were randomly allocated into four groups: Wild Type mice normal group (WT), Wild Type mice model group (WT + LPS), PLD2 gene knockout mice normal group (PLD2$^{-/-}$), PLD2 knockout mice model group (PLD2$^{-/-}$ + LPS). To establish an ALI animal model, WT + LPS and PLD2$^{-/-}$ + LPS mice were intraperitoneally injected 20 mg/kg LPS (L2880, Escherichia coli O55:B5, Sigma-Aldrich St. Louis, MO, USA). WT and PLD2$^{-/-}$ mice were intraperitoneally injected with the same amount of sterile normal saline. After LPS was administered in mice for 6h, all mice were intraperitoneally injected with 4% chloral hydrate. Lung tissues of mice were obtained after full anesthesia.

## 2.2 Histopathology and Lung Injury Score

Mouse lung tissues were collected and fixed with 4% paraformaldehyde for 48 h. The tissues were processed, embedded in paraffin, sectioned into 5-μm-thick slices, stained with hematoxylin and eosin (H&E) (Novland, Shanghai, China), and visualized under an optical microscope (Olympus Optical, Tokyo, Japan) for histological analysis. For each sample, six high-magnification fields were randomly scored for each feature, and the obtained mean was the pathological score of each sample following the lung injury score criteria [25].

## 2.3 Wet/dry (W/D) lung weight ratio

The lung was excised, blotted dry, weighed to obtain the wet weight, and then placed in an oven at 60◦C for 48 h to obtain the dry weight. The W/D ratio was used to evaluate the degree of pulmonary edema.

## 2.4 Cell culture

HUVECs were purchased from the Shanghai cell bank and cultured in a 5% CO2 incubator at 37ºC in a complete culture medium (AllCells, Shanghai, China). Cells were cultured to 85–90% confluency and passaged in 0.25% trypsin (containing 0.02% EDTA; Procell, Wuhan, China). The cells were also separated into four groups: control, LPS (10μg/ml), LPS + CAY10594 (PLD2 inhibitor) (10μmol/L; 1130067-34-3,

Cayman chemical, Michigan, USA), and CAY10594 group. In the experiment of adding exogenous PA, HUVECs were divided into four groups: control, PA (50μmol/L), PA + STAT3-IN-1 (STAT3 inhibitor) (5uM; Cat. No.Hy-100753, MedChemExpress, Shanghai, China), and STAT3-IN-1 group. The LPS, CAY10594 and STAT3-IN-1 group concentrations used were based on the results of preliminary experiments.

# 2.5 Assessment of HUVECs permeability

HUVECs were seeded at 15,000 cells per insert well and cultured for 1 to 3 d to allow for growth of a confluent monolayer. Cells were pretreated with CAY10594 (10μmol/L) for 1 h, followed by LPS treatment (10μg/ml) for 6 h. After treatment, Fluorescein isothiocyanate-dextran (FITC-dextran) (40842-46-8, Sigma-Aldrich St. Louis, MO, USA) with a final concentration of 2mg/ ml was added to the upper layer of the transwell chamber (3470, 6.5 mm Transwell® with 0.4 um Pore Polyester Membrane Insert, Costar, Massachusetts, USA ) and incubated at 37°C for 30min. 100 μl of medium was withdrawn from the lower well and upper well, respectively. Measurements were taken with a microplate reader using excitation and emission wavelengths of 490 and 525 nm, respectively. The permeability coefficient of endothelial cells was =[A]/ T × L /A× V /[L]. Where [A] is the fluorescence protein concentration in the lower chamber, t is the time, expressed in seconds, A is the filtration area, expressed in $cm^2$; V is the volume of liquid in the lower chamber; [L] is the concentration of fluorescent protein in the upper compartment [26].

# 2.6 Transendothelial Electrical Resistance

Briefly, Before the experiment begins, 300 μL of culture medium was added to the upper of transwell inserts, and 1ml of culture medium was added to the lower of transwell inserts. Two Millicell® ERS-2 (MERS00002, USA) resistance meter electrodes were placed on the surface and under the filter membrane. The basic resistance values of each compartment (blank resistance) were measured and HUVECs were seeded into each compartment at a density of 15,000 cells per well. After the cells fuse, cells were pretreated with CAY10594 (10μmol/l) for 1 h, followed by LPS treatment (10μg/ml) for 6 h. The resistance values of each compartment were then measured: ($\Omega/\square^2$) = (measured resistance - blank resistance) × effective membrane area [27, 28].

# 2.7 The content of PA in cell supernatant

After conducting different treatments and pretreatments of cells, a cell culture medium was collected, and the supernatant of each sample was collected after 3000 rpm under 4°C for 20 min. Thus, PA levels in the supernatant were evaluated with the ELISA kits (ml675014, Shanghai Enzymelinked Biotechnology Co., Ltd, Shanghai, China ) by the manufacturer's instructions.

# 2.8 Western Blot Analysis

After treatment, HUVECs and lung tissue proteins were extracted according to the requirements of the protein extraction kit (Cat#R0020 and Cat.No.P0100, Solarbio, Beijing, China), and protein concentrations in the supernatant were determined using a BCA Protein Assay kit (Cat.No.P0010S, Beyotime Biotechnology, Beijing, China). According to the different molecular weights of the target protein, the appropriate gel was prepared. Proteins were separated by SDS-PAGE (Cat.No.P0012A, Beyotime

Biotechnology, Beijing, China) and transferred to polyvinylidene fluoride (PVDF) (Cat. No.ISEQ00010, Merck Millipore, USA) membranes which were subsequently blocked with 5–7% skimmed milk for 2 h. Then the Membranes were incubated with primary antibodies against occludin (1:1000; 33-1500, Invitrogen, Carlsbad, CA, USA), ZO-1 (1:1000; ab276131, Abcam, Cambridge, UK), P-STAT3 (1:1000; ab32143, Abcam, Cambridge, UK), STAT3 (1:1500; ab68153, Abcam, Cambridge, UK), and β-actin (1:1000; 20536-1-AP, Proteintech, USA) overnight at 4℃, followed by incubation with horseradish peroxidase-conjugated antibodies (1:2000; Cat. No.SA00001-1 and Cat. No.SA00001-2, Proteintech, Chicago, USA) for 60 minutes at room temperature and protein bands were visualized by an electrochemiluminescence kit (MAO0186-1, Meilunbio, Dalian, China). Densitometry analysis was performed in the Image-J software.

# 2.9 Quantitative real-time PCR

Total RNA was isolated from HUVECs using Trizol Reagent (Ambion, Thermo, MA, USA) according to the manufacturer's protocol and the concentration and purity were detected on a nucleic acid analyzer. Total RNA was reverse transcribed and amplified by PCR using the Takara PrimeScript RT Reagent Kit ( RR037A, Takara, Shiga, Japan ). PCR reactions consisted of 12μL of PCR mix, 2μL cDNA, 1μL upstream primer, 1μL downstream primer, and qs to a final volume of 20 μL using ultrapure water. The reaction solution is prepared on ice. A two-step PCR procedure was used for detection and analysis by fluorescence quantitative PCR. mRNA expression was calculated using formula 2- (ΔCt sample– ΔCt control). The primer sequences are listed as follows. ZO-1 (Forward, 5’-ATAAAGTGCTGGCTTGGTCTGTTTG-3’ and Reverse, 5’-GCACTGCCCACCCATCTGTA-3’); occludin (Forward, 5’-ACTGGGTCAGGGAATATCCA-3’ and Reverse, 5’-TCAGCAGCAGCCATGTACTC-3’); GAPDH (Forward, 5’-GCACCGTCAAGGCTGAGAAC-3’ and Reverse, 5’-GCACTGCCCACCCATCTGTA-3’).

# 2.10 Immunofluorescence

The cells were inoculated on 24 well plates to detect the contents of occludin, and ZO-1 in HUVECs. HUVECs were fixed with 4% paraformaldehyde for 15 minutes and then blocked with goat serum for 1 h. After processing, the HUVECs were incubated with occludin (1:200) and ZO-1 (1:200) antibodies for 6 h. Next, a fluorescence secondary antibody (1:200; Cat #: A23220 and Cat #: A23420, Abbkine, California, USA) was added to the stain for 1h at room temperature. The samples were imaged by a fluorescence microscope, and the fluorescence intensity was quantitatively evaluated by image-J software.

To detect the contents of occludin and ZO-1 in lung tissues, lung tissues were sectioned into 5-μm-thick slices, lung specimens were sealed with goat serum after dewaxing and antigen repair. After processing, lung specimens were incubated with primary and secondary antibodies. the samples were imaged by fluorescence microscope. Finally, the sample is imaged with a fluorescence microscope.

### 2.11 Statistical analysis

All data were expressed as mean ± standard deviation (SD). One-way ANOVA was used to calculate differences between groups, and then the SNK test was performed. $p < 0.05$ was considered Statistically

significant. P-value□0.05 was considered Statistically significant. All statistical analyses were performed using IBM SPSS 25 software. All mathematical calculations and graphing were performed using GraphPad Prism 5.

# 3. Results

### 3.1 PLD2 deficiency can alleviate the histopathological changes of ALI mice and reduce the LPS-induced permeability of endothelial cells

Pulmonary edema and increased pulmonary vascular permeability are basic pathological features of ARDS. We investigated the effects of PLD2 on pulmonary edema and vascular permeability in LPS-induced ALI. Six hours after LPS intraperitoneal injection, lung tissue sections were stained with hematoxylin and eosin. The results showed that PLD2$^{-/-}$ significantly inhibited inflammatory cell infiltration and alveolar wall thickening. (Fig. 1. A, B), Furthermore, it effectively reduced the lung W/D ratio (Fig. 1. C). Using the Transwell chamber assay, we detected FITC-dextran and TEER transcellular resistance as indicators of HUVECs' relative permeability (Fig. 1. D, E). FITC-dextran, a branched glucose polymer, has no charge, is electrically neutral, and exhibits good biocompatibility. The advantage of this method is the fluorescence-based study of microcirculation and cell permeability. PLD2 inhibitor, CAY10594, exerted a protective effect on LPS-induced hyper-permeability. The results showed that CAY10594 could improve LPS-induced hyper-permeability compared to that in the LPS group, suggesting that CAY10594 could inhibit pulmonary capillary permeability.

## 3.2 PLD2 deficiency could protect occludin and ZO-1 damaged in ALI mice and LPS-induced HUVECs

Loss of endothelial barrier integrity is a common feature of LPS-induced ARDS. The results showed that changes in PLD2 expression after LPS induction were closely related to the endothelial barrier integrity. Tight junction protein expression in the lungs of control and PLD2$^{-/-}$ mice were analyzed. Western blot analysis showed that the expression of occludin and ZO-1 in the wild-type (WT) and PLD2$^{-/-}$ groups were higher and more consistent than that in the WT + LPS group. The expression of occludin and ZO-1 was significantly decreased, and the expression of these proteins was higher in the PLD2$^{-/-}$ + LPS group than in the WT + LPS group (Fig. 2. A-C). Additionally, the expression of occludin and ZO-1 in the same four groups was verified using immunofluorescence analysis (Fig. 2. D–G). This result suggests that PLD2 knockout protects the endothelial barrier integrity and enhances occludin and ZO-1 expression.

Because changes in PLD2 expression affect the expression of tight junction proteins in vivo, we evaluated whether similar changes occur in vitro. Western blotting and immunofluorescence analyses were used to detect the content of the main tight junction proteins occludin and ZO-1 in the control, LPS, LPS + CAY10594, and CAY10594 groups (Fig. 3. A-G). We observed that occludin and ZO-1 expression in the LPS group was significantly reduced, whereas the expression of these proteins in the LPS + CAY10594 group was higher than that in the LPS group. This is consistent with our data from mice. Additionally,

real-time quantitative polymerase chain reaction (RT-PCR) analysis showed consistent results, as verified by the gene expression (Fig. 3. H–I). In summary, our data indicate that PLD2 participates in the downregulation of occludin and ZO-1 expression in lung endothelial cells.

### 3.3 PLD2 expression and its catalytic product PA increased in LPS-induced mice and HUVECs, and PA further induces STAT3 phosphorylation

PLD2 hydrolyzes phosphatidylcholine to produce phosphatidic acid and choline. Under various upstream stimuli, PLD2 activation causes PA production to increase, which is considered a key event for initiating various cellular responses. Under the action of LPS, PA expression in the supernatant of HUVECs was detected using ELISA (Fig. 4. A). Compared to the LPS group, PA expression in the LPS + CAY10594 group was significantly reduced. Under the action of LPS, PLD2 enhanced the expression of PA, a catalytic product. Next, we investigated the mechanism by which PA promoted the destruction of tight junction proteins. In the in vivo experiments, we analyzed the expression of phosphorylated STAT3 in the lungs of mice in the LPS-induced control and PLD2 knockout groups. Western blot analysis showed that the expression of phosphorylated STAT3 in the WT + LPS group was significantly increased. Compared with that in the WT + LPS group, the expression of phosphorylated STAT3 in the $PLD2^{-/-}$ + LPS group was decreased (Fig. 4. B, C). The results of the in vitro experiments showed that the expression of phosphorylated STAT3 in the LPS group was significantly increased. In contrast, the expression of phosphorylated STAT3 in the LPS + CAY10594 group was lower than that in the LPS group (Fig. 4. D, E). To verify whether this result is PA-induced phosphorylation of STAT3, we analyzed the control group and the exogenously added PA group using western blotting (Fig. 4. F, G). We observed that the expression of phosphorylated STAT3 significantly increased in the PA group. This result shows that, under the action of LPS, PLD2 enhances PA expression, which is a catalytic product, and PA further induces STAT3 phosphorylation.

## 3.4 Inhibition of STAT3 phosphorylation attenuates PA-induced degradation of endothelial tight junctions

We detected the levels of the main tight junction proteins occludin and ZO-1 in the control, PA, PA + STAT3-IN-1, and STAT3-IN-1 HUVEC groups using western blotting and immunofluorescence analyses (Fig. 5. A–G). We observed that occludin and ZO-1 expression in the PA group was significantly reduced, and the expression of these proteins was higher in the PA + STAT 3-IN-1 group than in the PA group. In addition, RT-PCR analysis showed that the above results were verified based on the gene expression level (Fig. 5. H, I). In summary, our data indicate that inhibiting STAT3 phosphorylation attenuates the PA-induced degradation of endothelial tight junctions.

# 4. Discussion

In this study, we aimed to determine the role of PLD2 in the pathogenesis of ALI and to verify that PLD2 is an important endothelial permeability regulator. To this end, we used knockout mice to establish an

experimental LPS-induced ALI model. We used HUVECs to detect the effect of changes in PLD2 expression or changes in intracellular PA levels on endothelial permeability. Our results showed that knocking out PLD2 alleviated ALI in mice. Intracellular PA enhancement increases endothelial cell permeability, and PLD2 is specifically involved in regulating endothelial permeability. Our study revealed that the PLD2-dependent increase in endothelial cell permeability is related to the activation of PA and STAT3 signaling pathways. The STAT3 signaling pathway negatively regulates occludin and ZO-1 expression. This study highlights the novel role of PLD2 in regulating the tight junction proteins occludin and ZO-1 and the pulmonary endothelial barrier.

Much effort has been devoted to uncovering the function of PLD2 in specific situations, such as disease, which makes PLD2 function more predictable than expected [29]. Furthermore, because PLD2 is ubiquitously expressed in most cell types, more complex studies using knockout animal models are required to reveal the cell-, tissue-, and organ-specific functions of PLD2 [30]. PLD2 plays a role in various pathological conditions. Studies using PLD2 knockout mice have identified previously unknown functions of PLD2 in the pathology of several diseases [31]. Abdulnour et al. recently demonstrated that PLD2 expression is associated with mortality in patients with ARDS and that PLD2 expression is decreased in murine self-resolving ALI. PLD2 deficiency reduces ALI severity and is associated with the increased recruitment of macrophages with enhanced phagocytosis and decreased neutrophil production of reactive oxygen species (ROS) [29]. To our knowledge, the role of PLD2 in ARDS pathogenesis has not been elaborated [32]. Our results showed that PLD2 deletion improved lung integrity and prevented ALI in LPS-induced mice. In in vivo experiments, we found no significant difference in lung integrity and pulmonary vascular permeability between WT and $PLD2^{-/-}$ mice, whereas $PLD2^{-/-}$ + LPS significantly changed lung histopathology and decreased pulmonary vascular permeability than in WT + LPS mice. Similarly, in vitro chemical inhibition of PLD2 in HUVECs also reduced LPS-induced barrier permeability, suggesting that the PLD2 gene may play a significant role in the event of injury. As we observed increased paracellular permeability, the loss of tight junction proteins might be a predisposing factor for ARDS.

In ARDS, changes in tight junctions contribute to the development of pulmonary edema and the continuation of inflammation [8]. Since it is widely accepted that tight junctions play a central role in regulating the extracellular permeability of endothelial cells, the structure of endothelial tight junctions has been extensively studied [33]. Tight junctions are critical for lung barrier stability and have important clinical implications [12, 34]. In a mouse ALI model, where increased vascular permeability and vascular integrity disruption occurred during lung injury pathogenesis, PLD2 loss provided tight junction protein-related protection [17, 18]. Tight junctions provide paracellular permeability for solutes and macromolecules as structural barriers. The expression of the structural membrane proteins occludin, ZO-1, claudin-5, and JAM-A is related to tight junction permeability [35]. In our gene-null mice, LPS-induced reduction in occludin and ZO-1 levels was restored, indicating that PLD2 regulates occludin and ZO-1 expression under LPS action. There was an inverse relationship between PLD2, occludin, and ZO-1 expression. Occludin is a tetrameric membrane protein with two extracellular loops separated by short

intracellular loops. The carboxy- and amino-terminal domains are cytoplasmic and involved in various signaling pathways [36]. ZO-1 is a tight junction that provides para-cellular permeability to solutes and macromolecules as a structural barrier. The expression of the structural membrane proteins occludin, ZO-1, claudin-5, and JAM-A is related to the permeability of tight junctions [35]. The plaque protein binds to occludin in the cytoplasm and localizes occludin in the cytoskeleton to ensure tight junction integrity [7]. While claudin-5 and JAM-A are also essential components of tight junctions, claudin-5 exists in the para-cellular space and is highly expressed in ECs [33, 37]. Tight junctions function as a closure to restrict the passage of proteins, ions, and water through the intercellular space; as a fence to prevent the mixing of the apical and basolateral plasma membrane domains; and as a channel to regulate the passage of ions and water through the intercellular space [10, 12]. Our results confirm a novel role for PLD2 in regulating the tight junction proteins occludin and ZO-1. However, whether PLD2 also regulates other components of endothelial tight junction proteins (claudin-5 and JAM-A) remains unclear. In this study, we established that the genetic or pharmacological inhibition of PLD2 restored occludin and ZO-1 levels, alleviated ARDS symptoms, and improved mouse survival. The repair of tight junction proteins by inhibiting PLD2 could serve as a therapeutic intervention in patients with ARDS. Combining this therapy with conventional drugs may be a promising therapeutic strategy [32, 38].

We observed that after LPS-induced ARDS in mice, STAT3 phosphorylation was significantly increased in WT + LPS mice, whereas PLD2 inhibition attenuated phosphorylation. Similarly, we obtained the same results using the in vitro chemical inhibition of PLD2 in HUVECs. PLD2 is a lipid signal transduction enzyme whose classical function is to catalyze the hydrolysis of PC to generate the signal molecule PA [39]. We next tested whether the PA increase was positively related to STAT3 phosphorylation, confirming this hypothesis. This result suggests that regulating STAT3 by PLD2 may be mediated by PA.

Since PLD2 activity and levels are associated with STAT3 phosphorylation, it may also predict disease diagnosis and recurrence. In this study, we focused on the specific role of PLD2 in regulating tight junctions via a STAT3-dependent pathway. Our study shows that the PLD2-dependent increase in endothelial cell permeability is associated with activation of the PA and STAT3 signaling pathways. The STAT3 signaling pathway negatively regulates occludin and ZO-1 expression. Therefore, we showed that the STAT3 signaling pathway also plays a vital role in regulating occludin and ZO-1 and maintaining lung barrier integrity. However, further studies, including human tissue samples, are required to determine the role of PLD2 in regulating STAT3 in clinical pathogenesis and disease persistence.

This study had certain limitations. On the one hand, the effects of PLD2 on occludin and ZO-1 were studied at the cellular and mouse levels but not in higher animals. However, whether other signaling pathways involving occludin and ZO-1 proteins affect LPS-induced ARDS requires further investigation. Collectively, this study demonstrated that PLD2 deletion or inhibition significantly inhibits tight junction damage and alleviates lung injury. Although LPS-induced PA production can lead to STAT3 activation, further studies will help elucidate the detailed mechanism of LPS-induced PLD2 upregulation in ARDS.

# 5. Conclusions

Our study revealed that PLD2 expression and its catalytic product PA increased in LPS-induced mice and HUVECs, and PA further induced STAT3 phosphorylation. The STAT3 signaling pathway negatively regulates the expression of the tight junction proteins occludin and ZO-1. Therefore, our data suggest that blocking PLD2 can improve ALI, providing a new theoretical and experimental basis for the clinical application of PLD2 in ARDS (Fig. 6).

# Abbreviations

ARDS: Acute respiratory distress syndrome; ALI: Acute lung injury; PA :phosphatidic acid; PLD2: Phospholipase D2; PA: Phosphatidic acid; HUVECs: Human umbilical vein endothelial cells; DAD: Diffuse alveolar damage; ZO-1: zonula occludens protein-1; PC: Phosphatidylcholine; STAT: Signal transducer and activator of transcription; FITC-dextran: Fluorescein isothiocyanate-dextran; ROS: reactive oxygen species.

# Declarations


### Acknowledgements

Not applicable


Author contributions

Conceived and designed the experiments: XZW, XH, BYQ, TTQ. Performed the experiments: TTQ, BYQ, YXF, LJ, YTS. Analyzed the data: TTQ, LQL, SRS, BJL. Contributed reagents/materials/analysis tools: XZW, XH. Wrote the manuscript: TTQ, XH. All authors read and approved the final manuscript.


### Funding

This study was supported by National Natural Science Foundation of China (grant no. 81670078), Taishan Scholar Project of Shandong Province, Key Clinical Specialty Project of Shandong Province.


### Availability of data and materials

The datasets supporting the conclusions of this article are included within the article.

### Ethics approval and consent to participate.

All the mice were fed and used according to the NIH guidelines, and this study was approved by the Ethics Committees on Animal Experimentation of Binzhou Medical University

### Consent for publication

Not applicable.

### Competing interests

The authors declare that they have no conflict of interest.


### Author details

[1] Department of Intensive Care Unit, Binzhou Medical University Hospital, Binzhou, Shandong, China.

[2] Cardiac Surgical Intensive Care Unit, Yantai yuhuangding Hospital of Qingdao University Medical College, Yantai, Shandong, China.

[3] Department of Pulmonary and Critical Care Medicine, Yantai Affiliated Hospitol of Binzhou Medical University, Yantai, Shandong, China.

[4] Department of Hematology, Binzhou Medical University Hospital, Binzhou, Shandong, China.


# References


1. Morales-Ortíz J, Deal V, Reyes F, et al. Platelet-derived TLT-1 is a prognostic indicator in ALI/ARDS and prevents tissue damage in the lungs in a mouse model. Blood. 2018;132(23):2495–2505. doi:10.1182/blood-2018-03-841593
2. Bernard G. Acute Lung Failure - Our Evolving Understanding of ARDS. N Engl J Med. 2017;377(6):507–509. doi:10.1056/NEJMp1706595
3. Matthay MA, Zemans RL, Zimmerman GA, et al. Acute respiratory distress syndrome. Nat Rev Dis Primers. 2019;5(1):18. Published 2019 Mar 14. doi:10.1038/s41572-019-0069-0
4. Luyt CE, Bouadma L, Morris AC, et al. Pulmonary infections complicating ARDS. Intensive Care Med. 2020;46(12):2168–2183. doi:10.1007/s00134-020-06292-z
5. Stevens JP, Law A, Giannakoulis J. Acute Respiratory Distress Syndrome. JAMA. 2018;319(7):732. doi:10.1001/jama.2018.0483
6. Takahashi Y, Kawasaki T, Sato H, et al. Functional Roles for CD26/DPP4 in Mediating Inflammatory Responses of Pulmonary Vascular Endothelial Cells. Cells. 2021;10(12):3508. Published 2021 Dec 11. doi:10.3390/cells10123508
7. Umeda K, Ikenouchi J, Katahira-Tayama S, et al. ZO-1 and ZO-2 independently determine where claudins are polymerized in tight-junction strand formation. Cell. 2006;126(4):741–754. doi:10.1016/j.cell.2006.06.043
8. Li J, Qi Z, Li D, et al. Alveolar epithelial glycocalyx shedding aggravates the epithelial barrier and disrupts epithelial tight junctions in acute respiratory distress syndrome. Biomed Pharmacother. 2021;133:111026. doi:10.1016/j.biopha.2020.111026
9. Chen L, Li L, Han Y, Lv B, Zou S, Yu Q. Tong-fu-li-fei decoction exerts a protective effect on intestinal barrier of sepsis in rats through upregulating ZO-1/occludin/claudin-1 expression. J Pharmacol Sci.

2020;143(2):89–96. doi:10.1016/j.jphs.2020.02.009

10. Guttman JA, Samji FN, Li Y, Vogl AW, Finlay BB. Evidence that tight junctions are disrupted due to intimate bacterial contact and not inflammation during attaching and effacing pathogen infection in vivo. Infect Immun. 2006;74(11):6075–6084. doi:10.1128/IAI.00721-06
11. Zhang D, Zhang JT, Pan Y, et al. Syndecan-1 Shedding by Matrix Metalloproteinase-9 Signaling Regulates Alveolar Epithelial Tight Junction in Lipopolysaccharide-Induced Early Acute Lung Injury. J Inflamm Res. 2021;14:5801–5816. Published 2021 Nov 4. doi:10.2147/JIR.S331020
12. Herrero R, Prados L, Ferruelo A, et al. Fas activation alters tight junction proteins in acute lung injury. Thorax. 2019;74(1):69–82. doi:10.1136/thoraxjnl-2018-211535
13. Feng J, Pan W, Yang X, et al. RBM3 Increases Cell Survival but Disrupts Tight Junction of Microvascular Endothelial Cells in Acute Lung Injury. J Surg Res. 2021;261:226–235. doi:10.1016/j.jss.2020.12.041
14. Jenkins GM, Frohman MA. Phospholipase D: a lipid centric review. Cell Mol Life Sci. 2005;62(19–20):2305–2316. doi:10.1007/s00018-005-5195-z
15. Ghim J, Chelakkot C, Bae YS, Suh PG, Ryu SH. Accumulating insights into the role of phospholipase D2 in human diseases. Adv Biol Regul. 2016;61:42–46. doi:10.1016/j.jbior.2015.11.010
16. Fu P, Ramchandran R, Shaaya M, et al. Phospholipase D2 restores endothelial barrier function by promoting PTPN14-mediated VE-cadherin dephosphorylation. J Biol Chem. 2020;295(22):7669–7685. doi:10.1074/jbc.RA119.011801
17. Chelakkot C, Ghim J, Rajasekaran N, et al. Intestinal Epithelial Cell-Specific Deletion of PLD2 Alleviates DSS-Induced Colitis by Regulating Occludin. Sci Rep. 2017;7(1):1573. Published 2017 May 8. doi:10.1038/s41598-017-01797-y
18. Zeiller C, Mebarek S, Jaafar R, et al. Phospholipase D2 regulates endothelial permeability through cytoskeleton reorganization and occludin downregulation. Biochim Biophys Acta. 2009;1793(7):1236–1249. doi:10.1016/j.bbamcr.2009.04.001
19. Zou S, Tong Q, Liu B, Huang W, Tian Y, Fu X. Targeting STAT3 in Cancer Immunotherapy. Mol Cancer. 2020;19(1):145. Published 2020 Sep 24. doi:10.1186/s12943-020-01258-7
20. Hillmer EJ, Zhang H, Li HS, Watowich SS. STAT3 signaling in immunity. Cytokine Growth Factor Rev. 2016;31:1–15. doi:10.1016/j.cytogfr.2016.05.001
21. Kim YR, Byun HS, Won M, et al. Modulatory role of phospholipase D in the activation of signal transducer and activator of transcription (STAT)-3 by thyroid oncogenic kinase RET/PTC. BMC Cancer. 2008;8:144. Published 2008 May 23. doi:10.1186/1471-2407-8-144
22. Yu H, Lee H, Herrmann A, Buettner R, Jove R. Revisiting STAT3 signalling in cancer: new and unexpected biological functions. Nat Rev Cancer. 2014;14(11):736–746. doi:10.1038/nrc3818
23. Thilakasiri PS, Dmello RS, Nero TL, Parker MW, Ernst M, Chand AL. Repurposing of drugs as STAT3 inhibitors for cancer therapy. Semin Cancer Biol. 2021;68:31–46. doi:10.1016/j.semcancer.2019.09.022

24. Zhang J, Luo Y, Wang X, et al. Global transcriptional regulation of STAT3- and MYC-mediated sepsis-induced ARDS. Ther Adv Respir Dis. 2019;13:1753466619879840. doi:10.1177/1753466619879840
25. Aeffner F, Bolon B, Davis IC. Mouse Models of Acute Respiratory Distress Syndrome: A Review of Analytical Approaches, Pathologic Features, and Common Measurements. Toxicol Pathol. 2015;43(8):1074–1092. doi:10.1177/0192623315598399
26. Chen QH, Liu AR, Qiu HB, Yang Y. Interaction between mesenchymal stem cells and endothelial cells restores endothelial permeability via paracrine hepatocyte growth factor in vitro. Stem Cell Res Ther. 2015;6(1):44. Published 2015 Mar 24. doi:10.1186/s13287-015-0025-1
27. Eaton AD, Zimmermann C, Delaney B, Hurley BP. Primary human polarized small intestinal epithelial barriers respond differently to a hazardous and an innocuous protein. Food Chem Toxicol. 2017;106(Pt A):70–77. doi:10.1016/j.fct.2017.05.038
28. Luo L, Liu S, Zhang D, et al. Chromogranin A (CGA)-derived polypeptide (CGA47-66) inhibits TNF-α-induced vascular endothelial hyper-permeability through SOC-related Ca2 + signaling. Peptides. 2020;131:170297. doi:10.1016/j.peptides.2020.170297
29. Hwang WC, Seo SH, Kang M, et al. PLD1 and PLD2 differentially regulate the balance of macrophage polarization in inflammation and tissue injury. J Cell Physiol. 2021;236(7):5193–5211. doi:10.1002/jcp.30224
30. Abdulnour RE, Howrylak JA, Tavares AH, et al. Phospholipase D isoforms differentially regulate leukocyte responses to acute lung injury. J Leukoc Biol. 2018;103(5):919–932. doi:10.1002/JLB.3A0617-252RR
31. Ghim J, Moon JS, Lee CS, et al. Endothelial deletion of phospholipase D2 reduces hypoxic response and pathological angiogenesis. Arterioscler Thromb Vasc Biol. 2014;34(8):1697–1703. doi:10.1161/ATVBAHA.114.303416
32. Lee SK, Kim SD, Kook M, et al. Phospholipase D2 drives mortality in sepsis by inhibiting neutrophil extracellular trap formation and down-regulating CXCR2. J Exp Med. 2015;212(9):1381–1390. doi:10.1084/jem.20141813
33. Jia Y, Qin T, Zhang X, et al. Effect of bevacizumab on the tight junction proteins of vascular endothelial cells. Am J Transl Res. 2019;11(9):5546–5559. Published 2019 Sep 15.
34. Kurihara H, Anderson JM, Farquhar MG. Diversity among tight junctions in rat kidney: glomerular slit diaphragms and endothelial junctions express only one isoform of the tight junction protein ZO-1. Proc Natl Acad Sci U S A. 1992;89(15):7075–7079. doi:10.1073/pnas.89.15.7075
35. Suzuki R, Nakamura Y, Chiba S, et al. Mitigation of tight junction protein dysfunction in lung microvascular endothelial cells with pitavastatin. Pulm Pharmacol Ther. 2016;38:27–35. doi:10.1016/j.pupt.2016.04.003
36. Torres-Flores JM, Silva-Ayala D, Espinoza MA, López S, Arias CF. The tight junction protein JAM-A functions as coreceptor for rotavirus entry into MA104 cells. Virology. 2015;475:172–178. doi:10.1016/j.virol.2014.11.016

37. Dilling C, Roewer N, Förster CY, Burek M. Multiple protocadherins are expressed in brain microvascular endothelial cells and might play a role in tight junction protein regulation. J Cereb Blood Flow Metab. 2017;37(10):3391–3400. doi:10.1177/0271678X16688706
38. Zhou G, Yu L, Yang W, Wu W, Fang L, Liu Z. Blockade of PLD2 Ameliorates Intestinal Mucosal Inflammation of Inflammatory Bowel Disease. Mediators Inflamm. 2016;2016:2543070. doi:10.1155/2016/2543070
39. Wang Z, Cai M, Tay LWR, et al. Phosphatidic acid generated by PLD2 promotes the plasma membrane recruitment of IQGAP1 and neointima formation. FASEB J. 2019;33(6):6713–6725. doi:10.1096/fj.201800390RR

# Figures

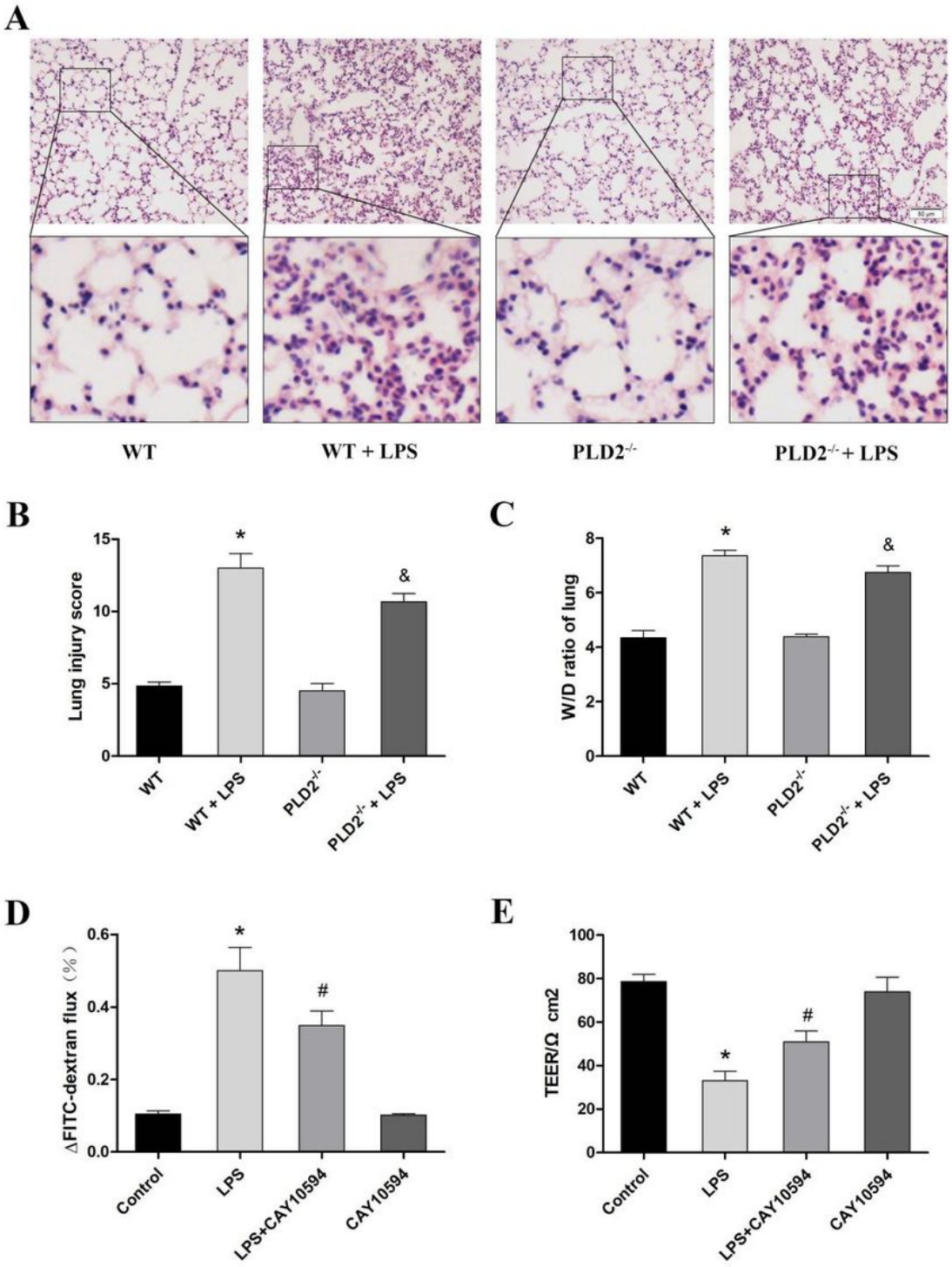


## Figure 1

**Effects of PLD2 expression on histopathological changes and lung wet-dry ratio in LPS induced ALI mice and endothelial permeability.** After 6 h of the LPS (20mg/kg) challenge, lung tissues from each experimental group were processed for histological evaluation. (n = 6mice/group; magnification 200×, scale bar: 50μm) (A, B), and the lung W/D ratio (C). The effect of PLD2 on the permeability of HUVECs treated with LPS was assessed using FITC-dextran and TEER methods (E). All data are presented as the

mean ± SD of three independent experiments. *p < 0.05 vs the control group. &p < 0.05 vs the WT + LPS group . #p < 0.05 vs the LPS group.

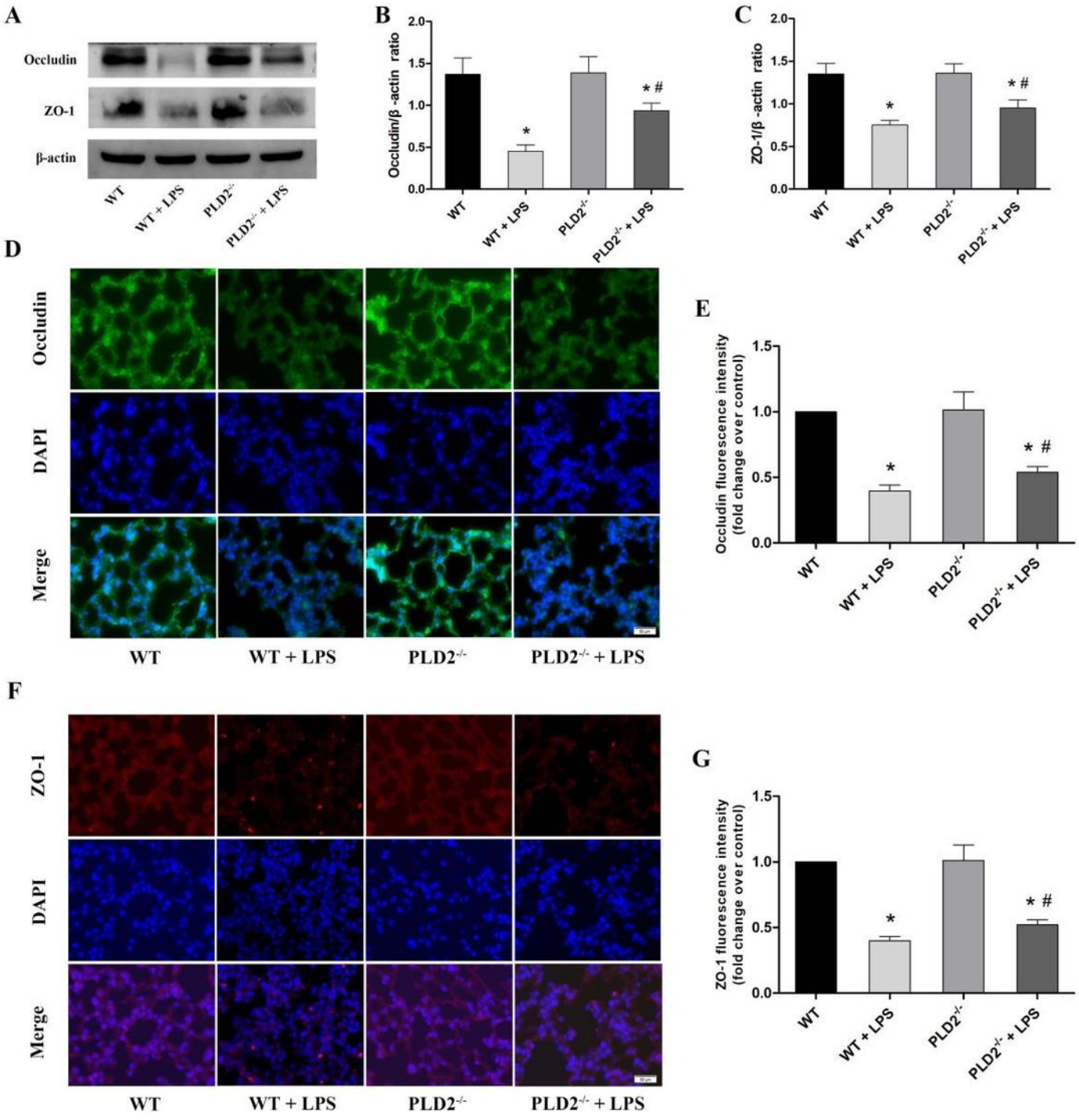


## Figure 2

**Effects of PLD2 expression on LPS induced pulmonary occludin and ZO-1 in ALI mice.** After 6 h of LPS (20mg/kg) challenge, lung tissues were obtained for occludin and ZO-1 expression. The proteins of

occludin, ZO-1and β-actin were detected by the Western blot (A). The β-actin was used as the internal control. Quantification of occludin and ZO-1 are shown in (B) and (C) respectively. Distributions of occludin (D) and ZO-1 (F) and associated fluorescence intensity analysis of occludin (E) and ZO-1 (G) in the lungs of mice in the WT, WT + LPS, PLD2$^{-/-}$, and PLD2$^{-/-}$ + LPS groups. (magnification × 200; scale bar, 50 μm) .All data are presented as the mean ± SD of three independent experiments. *p < 0.05 vs the WT group. #p < 0.05 vs WT + LPS group.

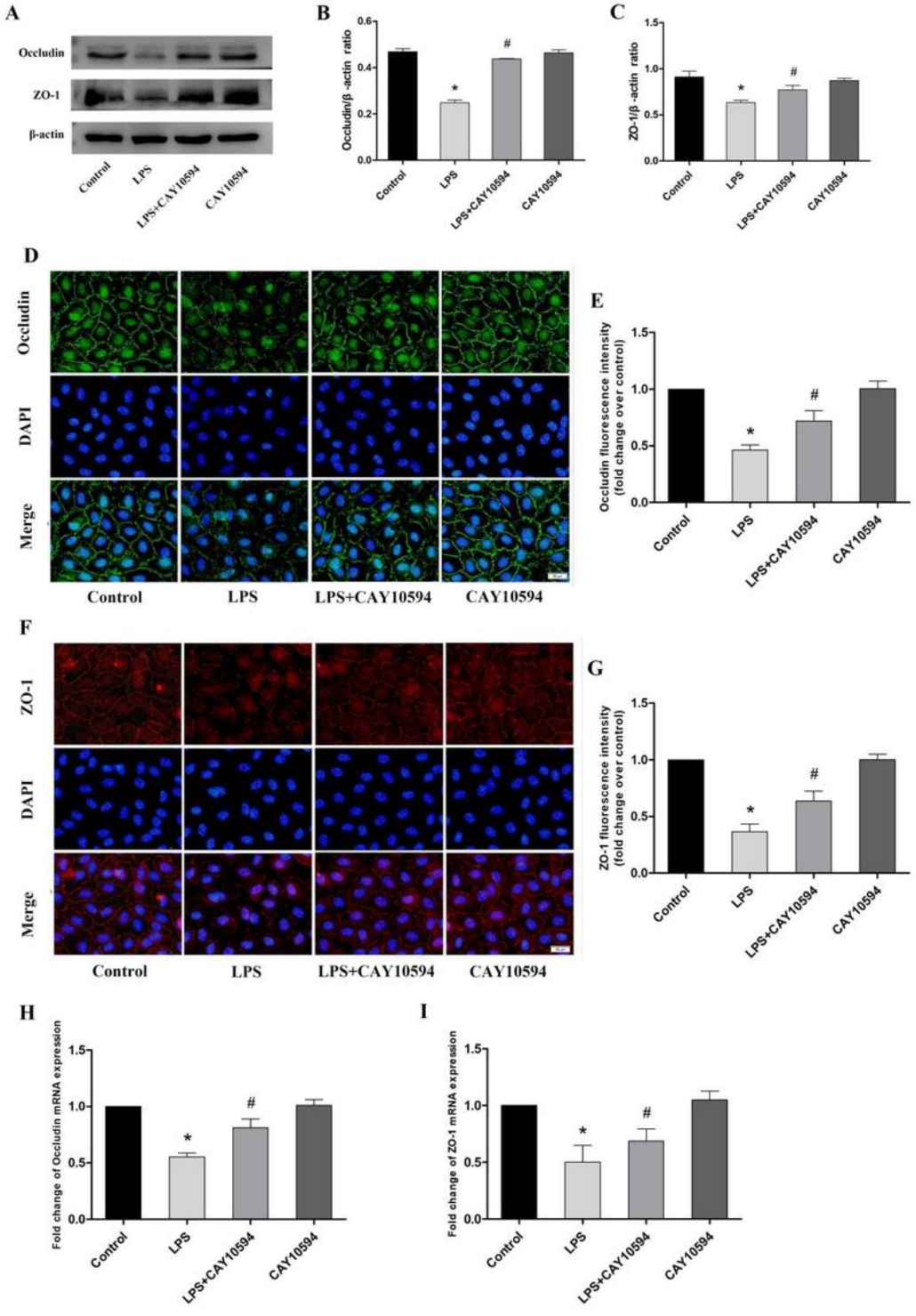

## Figure 3

**The effect of PLD2 expression on occludin and ZO-1 in HUVECs.** After 6 h of LPS (10μg/ml) challenge, Western blotting analysis of occludin and ZO-1 in HUVECs in the control, LPS, LPS + CAY10594 and CAY10594 groups (A). The β-actin was used as the internal control. Quantification of occludin and ZO-1 are shown in (B) and (C) respectively. Immunofluorescence images to determine occludin (D) and ZO-1 (F) levels in HUVECs from each group. (magnification × 200; scale bar, 50 μm) . Quantification of occludin and ZO-1 are shown in (E) and (G) respectively. mRNA levels of occludin and ZO-1 in the HUVECs were evaluated via qRT-PCR (H, I). All data are presented as the mean ± SD of three independent experiments. *p < 0.05 vs the Control group. #p < 0.05 vs the LPS group.

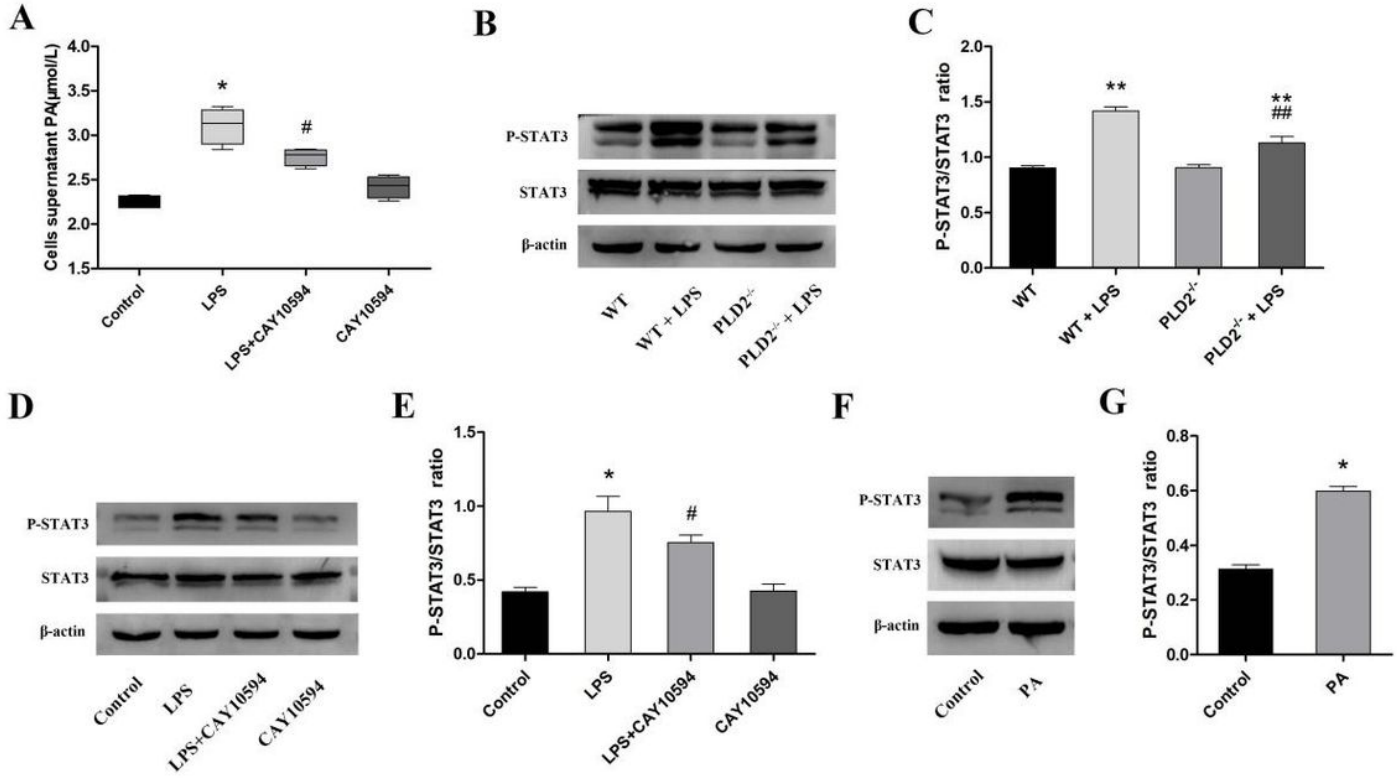


## Figure 4

**PLD2 enhanced the expression of PA and the effect of PLD2/PA on STAT3.** PA in the cell supernatant of the cell was evaluated using ELISA (A). After 6 h of LPS (20mg/kg) challenge, lung tissues were obtained for P-STAT3 and STAT3 expression. Western blotting analysis of P-STAT3 and STAT3 in the lungs of mice in the WT, WT + LPS, PLD2$^{-/-}$, and PLD2$^{-/-}$ + LPS groups (B). Quantification of P-STAT3 is shown in (C). After 6 h of LPS (10μg/ml) challenge, Western blotting analysis of P-STAT3 and STAT3 in HUVECs cells in the control, LPS, LPS + CAY10594 and CAY10594 groups (D). The β-actin was used as the internal control. Quantification of P-STAT3 is shown in (E). After 6 h of PA (50μmol/L) challenge, Western blotting analysis of P-STAT3 and STAT3 in HUVECs in the control and PA groups (F). The β-actin was used as the internal control. Quantification of P-STAT3 is shown in (G). All data are presented as the mean ± SD of

three independent experiments. *p < 0.05 vs the Control group. #p < 0.05 vs the LPS group.**p < 0.05 vs the WT group. ##p < 0.05 vs the WT + LPS group.

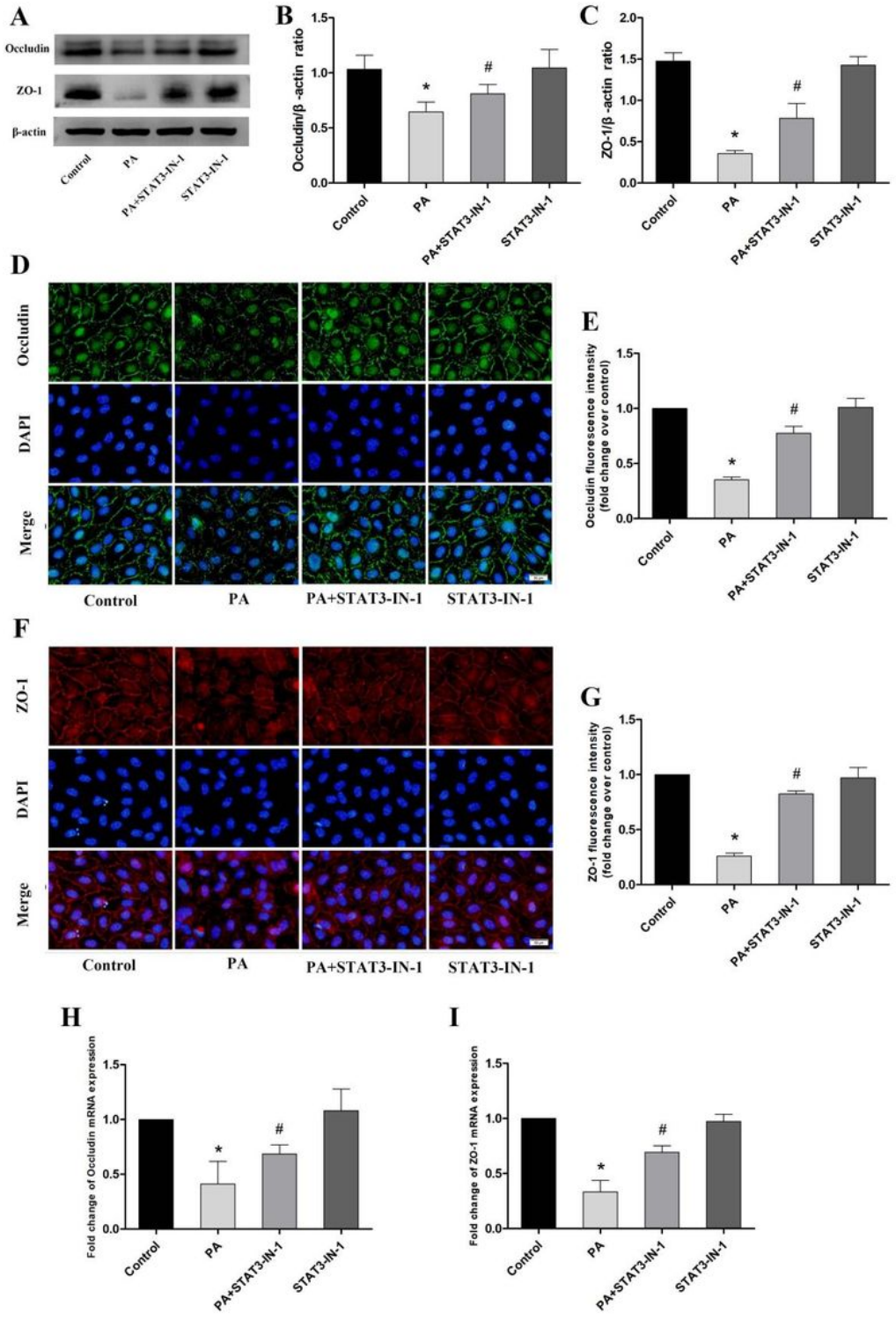


## Figure 5

**Effects of PA induced STAT3 phosphorylation on occludin and ZO-1 in HUVECs.** After 6 h of LPS (10μg/ml) challenge, Western blotting analysis of occludin and ZO-1 in HUVECs in the control, PA,

PA+STAT3-IN-1, and STAT3-IN-1 groups (A). The β-actin was used as the internal control. Quantification of occludin and ZO-1 are shown in (B) and (C) respectively. Immunofluorescence images to determine occludin (D) and ZO-1 (F) levels in HUVECs from each group. (magnification × 200; scale bar, 50 μm) . Quantification of occludin and ZO-1 are shown in (E) and (G) respectively. mRNA levels of occludin and ZO-1 in the HUVECs were evaluated via qRT-PCR (H, I). All data are presented as the mean ± SD of three independent experiments. *p < 0.05 vs the Control group. #p < 0.05 vs PA group.

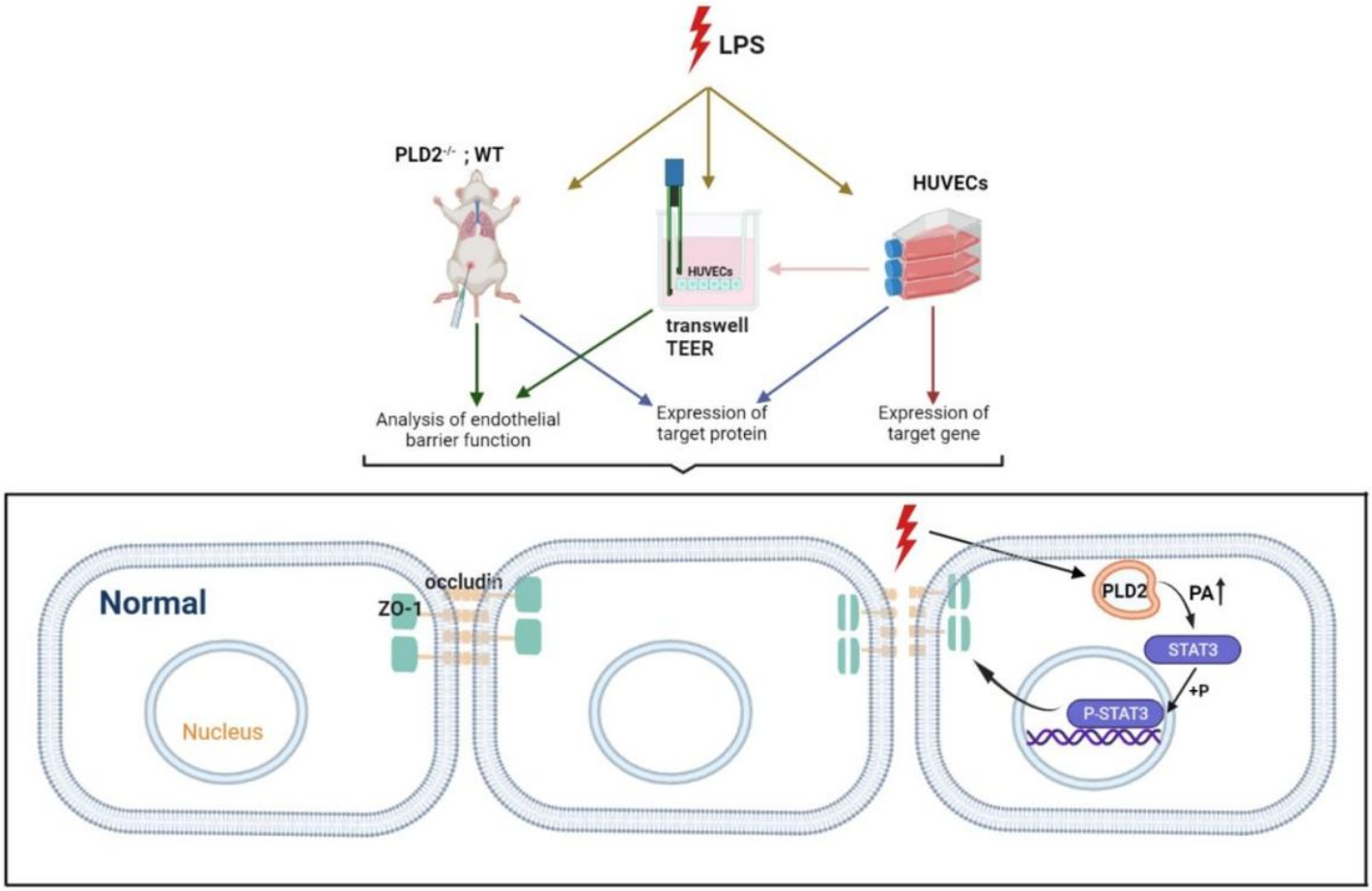


**Figure 6**

**Mechanisms by which PLD2 regulates lung endothelial barrier integrity.** LPS can up-regulate the expression of PLD2 in lung endothelial cells, PLD2 enhances the expression of the catalytic product PA, and PA further induces the transient activation (mainly through phosphorylation) of STAT3, which transmits transcriptional signals from cytokine and growth factor receptors on the cytoplasmic membrane to the nucleus to interact with occludin and ZO-1. Phosphorylated STAT3 signals and targets the tight junction proteins for disruption of occludin and ZO-1 therein, resulting in increased barrier permeability and thus increased inflammation. Illustrations are drawn using images from Bio RENDER, with minor modifications.

# Supplementary Files

This is a list of supplementary files associated with this preprint. Click to download.

- additionalfile.docx